Universiteit
Leiden
The Netherlands

In vivo magnetic resonance imaging and spectroscopy of Alzheimer__s disease in transgenic mice

Braakman, N.

Citation
Braakman, N. (2008, December 10). *In vivo magnetic resonance imaging and spectroscopy of Alzheimer__s disease in transgenic mice*. Retrieved from https://hdl.handle.net/1887/13328

Version:	Corrected Publisher's Version
License:	Licence agreement concerning inclusion of doctoral thesis in the Institutional Repository of the University of Leiden
Downloaded from:	https://hdl.handle.net/1887/13328

Note: To cite this publication please use the final published version (if applicable).

1 General introduction*

1.1 Alzheimer's disease

Alzheimer's disease is the most common neurodegenerative disease, the exact cause of which is still unknown. AD increases in incidence exponentially with age and is therefore poised to become a leading health problem as the population ages. The disease is characterized by a disruption of the neuronal function, progressive memory loss and gradual cognitive, functional and behavioral deterioration (1,2).

The two most prominent pathological features of AD are the extracellular senile plaques, and intracellular neurofibrillary tangles (Fig. 1.1) (1). Senile plaques consist of aggregated amyloid β protein, and are located mainly in the hippocampus, cerebral cortex and other areas of the brain essential for cognitive function. Neurofibrillary tangles consist of the hyperphosphorylated form of the microtubule associated protein tau. As the tau starts to form neurofibrillary tangles, it loses its cytoskeleton stabilizing function, leading to a collapse of the supporting structures in the neurons (Fig. 1.1). Other pathological features of the disease include neuronal cell loss, microglial activation, gross cerebral atrophy and synapse loss. Synaptic alterations and loss are considered by some investigators to be the most likely cause of the observed clinical symptoms (2).

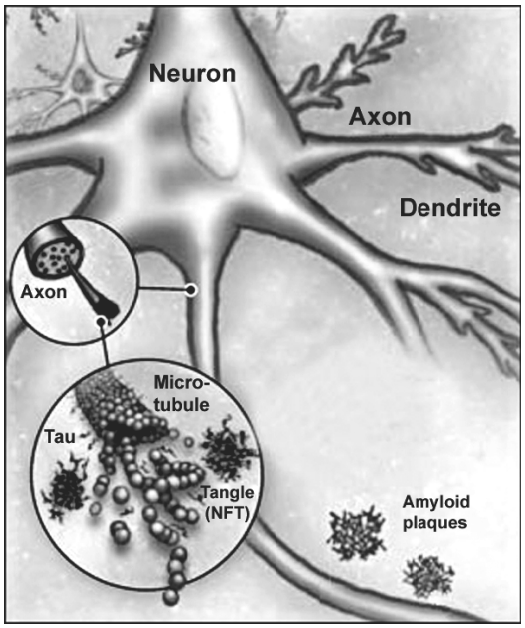

Fig. 1.1. Pathology of AD. Senile plaques that consist of Aβ are located extracellularly, while neurofibrillary tangles consisting of hyperphosphorylated tau are located intracellulary in AD brain.

The core of senile plaques consists mainly of aggregated amyloidogenic peptide Aβ, a highly hydrophobic peptide that spontaneously aggregates *in vitro* (3). The amyloid β protein is a 39- to 43-amino acid protein derived from the amyloid protein precursor through proteolytic cleavage by β- and γ-secretases (4,5). Soluble Aβ is a product of normal cell metabolism, and found in various body fluids including blood and

*Parts of this chapter were submitted to Curr Alzheimer Res

cerebrospinal fluid. Recent studies have shown that in AD brain, Aβ protein with 42 amino acid residues ($A\beta_{1-42}$) is deposited first and is the predominant form in senile plaques, while Aβ protein with 40 amino acid residues ($A\beta_{1-40}$) is deposited later in the disease and is prominent in vascular amyloid deposits (6). During aggregation, single monomeric Aβ peptides bind together to form oligomeric strings that assemble into fibrillar sheets. Multiple fibrils bind to form the backbone of the amyloid plaque, trapping other macromolecules along the way. There is recent consensus that the disordered metabolism of Aβ is central to the pathological cascade that ultimately leads to clinical AD, although the presence of Aβ plaques does not correlate well with neuronal loss and the onset, progress, or severity of dementia (7,8). The wide variety of mouse models of AD currently available (see section 1.2) has helped validate the assumed close relationship between Aβ accumulation and the formation of neurofibrillary pathology and neurodegeneration (4). Fig. 1.2 shows a recently proposed scheme of the interaction between Aβ and microtubule associated protein tau in AD pathogenesis (4).

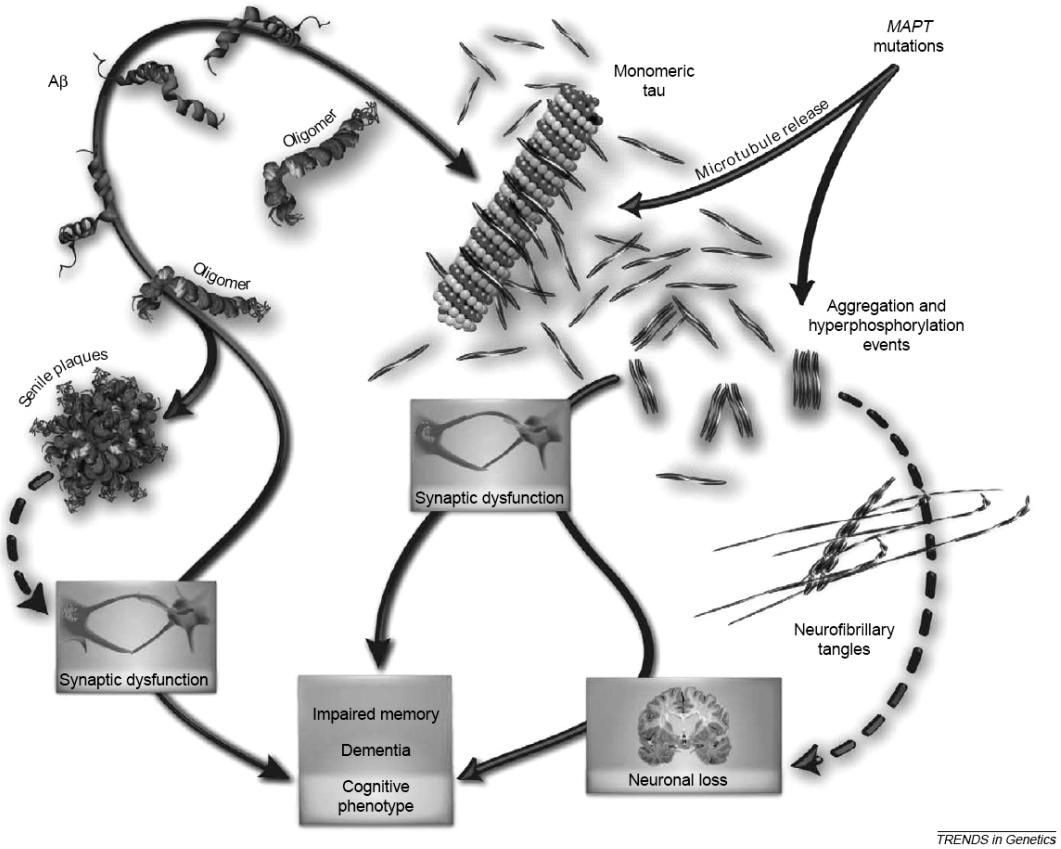

Fig. 1.2. The interaction of Aβ and microtubule associated protein tau (MAPT) in AD pathogenesis. In this scheme, accumulation of aggregated Aβ oligomers accelerates the parallel process of the formation of MAPT pathology. The toxic MAPT species then initiates neurodegeneration. Reprinted, with permission, from McGowan et al. 2006 (4). © Elsevier Ltd.

In this scheme, Aβ monomers can form soluble oligomeric species that cause synaptic dysfunction but do not lead directly to neuronal cell death (9). Aβ oligomers also aggregate to form senile plaques, and these dense cored structures have been shown to cause synaptic degeneration directly (10,11). In addition to a direct impact on synaptic activity, soluble Aβ oligomers can target MAPT pathogenesis, causing an acceleration of MAPT aggregation to form NFT with associated hyperphosphorylation (12). However, the major MAPT toxic species is not NFT. Earlier stage aggregates or modified monomers that appear to initially cause the reversible neuronal, or perhaps synaptic, dysfunction. Increasing accumulation leads to neuronal loss and permanent effects on cognitive phenotype (13).

The amyloid in senile plaques forms spherical cores that can range from 2 to ~200 μm, and are typically 20-60 μm in diameter (14). Aβ plaque formation precedes disease onset by many years and is generally accepted as a biomarker for onset and progression of the AD (7,15). Consequently, amyloid reduction in humans is now a major therapeutic objective. The map of plaque deposition established from post-mortem tissue samples indicates that amyloid is initially deposited in the basal temporal neocortex or entorhinal cortex. Deposition is then extended through the hippocampal formation and, in the final stage, to virtually all cortical areas, including the highly myelinated areas of the neocortex (16,17). However, establishment of the true map of plaque deposition as the disease progresses in living subjects is difficult due to lack of *in vivo* imaging methods for visualizing the development of Aβ plaques in humans.

Currently there is no definitive diagnosis for AD, except by post-mortem observation of senile plaques and neurofibrillary tangles and by eliminating other neurodegenerative disorders. The ability to visualize plaques or neurofibrillary tangles with an *in vivo* imaging technique coupled with clinical diagnosis would add a large degree of confidence to the diagnosis of AD. Non-invasive rapid visualization of Aβ plaques and identification of new early biomarkers of AD would not only facilitate intervention and enhance treatment success but also contribute toward understanding the mechanism of Alzheimer's disease.

1.2 Alzheimer mouse models

The main link between AD and Aβ is based on genetic mutations which were discovered in familial forms of AD and result in increased levels and deposition of Aβ. The three known classes of mutations associated with early onset, or familial AD all directly affect

amyloid metabolism and are: (a) mutations associated with the APP gene; (b) mutations associated with presenilin 1; and (c) mutations associated with presenilin 2. Presenilins are part of the γ-secretase protein complex, an internal protease that cleaves within the membrane-spanning domain of its substrate proteins, including APP (4). Transgenic mouse models of AD have been created by inserting one or more of these human mutations into the mouse genome (4,18,19). These transgenic mice display extensive amyloid plaque formation, while plaques are not found in the corresponding wild-type mice (15,20). Different strains of transgenic AD mice develop plaques at different rates (15,20). However, despite the amyloid deposition observed in these models, none of them develops widespread neuronal loss (21,22). Recently transgenic mice with MAPT mutations have also been developed. These mice develop neurofibrillary tangles similar to humans, coupled with neuronal losses in the affected brain regions (13,23,24). Several groups have combined APP, PS1, PS2 and/or MAPT mutations to generate double or triple transgenic mice. In these mice it was observed that Aβ deposition precedes neurofibrillary tangle development by several months, and furthermore that neurofibrillary tangle pathology was enhanced compared to MAPT-only transgenic mice (12,25,26). These findings suggest that Aβ accumulation can accelerate, if not initiate, the formation of neurofibrillary tangle pathology (12,27,28). A brief overview of the most commonly used transgenic mouse models of AD is given in Table 1.1.

Among the various commonly used mouse models, Tg2576 (19) is one of the most widely used models. This model over-expresses a human APP cDNA transgene with the K670M/N671L double mutation (APP_{swe} or Swedish mutation from the location of the family where the gene was originally identified). Tg2576 mice develop plaques starting at ~9 months of age and show memory deficits. The plaque distribution is primarily in the cortex and hippocampus, and, at later ages, is quite pronounced in the cingulate cortex. Tg2576 mice were used in the studies presented in chapters 3 and 5 of this thesis.

Table 1.1: Overview of the most commonly used mouse models in AD research

Model name	Transgene *(mutation)*	Cognitive deficits	Age of onset: Pathology	reference
Tg2576	APP *(APP_{695})*	Impaired reference and working memory, OR, CFC	9-11 months: Aβ plaques, astrogliosis, microgliosis, increased oxidative stress, dystrophic neurites	(19)
APP23	APP *(APP_{751})*	Impaired: reference memory, passive avoidance. Abnormal reflexes and stereotypic behavior, seizures	6 months: Aβ plaques, neuronal loss in CA1 region of hippocampus	(29)
$PS1_{M146V}$, $PS1_{M146L}$	PS1 *($PS1_{M146V}$, $PS1_{M146L}$)*	No behavioral abnormalities	No abnormal pathology; elevated Aβ42, altered mitochondrial activity, disregulation of calcium homoeostasis in $PS1_{M146V}$	(30)
PSAPP	APP/PS1 *($PS1_{M146L}$, APP_{695} PS1-A246E, APP_{695})*	Impaired reference and working memory	6-9 months: (accelerated) Aβ deposition, gliosis, dystrophic neurites	(18,31)
JNPL3	Tau *(Tau_{P301L})*	Not reported; Mice show progressing motor impairment with age	NFTs in spinal cord, spinal cord atrophy, astrocytosis in spinal cord, brain stem, diencephalon and telencephalon	(24)
Tau_{P301S}	Tau *(Tau_{P301S})*	Not reported	NFTs, severe paralysis of lower limbs due to motor neuron loss	(23)
Tau_{V337M}	Tau *(Tau_{V337M})*	Increased locomotor activity, deficits in plus maze	NFTs and neuronal degradation in hippocampus	(32)
Tau_{R406W}	Tau *(Tau_{R406W})*	Impaired associative memory in CFC, abnormality in PPI	Accumulation of insoluble tau, hyperphosphorylated tau inclusions in forebrain	(33)
rTg4510	Tau *(Tau_{P301L})*	Spatial defects, cognitive effects early. At 9.5 months exhibit decreased ambulation, body weight, hunched posture	Progressive age-related NFTs, neuronal loss and forebrain atrophy	(13,34)
Htau	Tau *(Human Tau)*	Not reported	NFTs and neuronal death	(35)
TAPP	APP/Tau *(APP_{695}, Tau_{P301L})*	Not reported	Aβ plaques, NFTs, gliosis	(12)
3×TgAD	APP/Tau/PS1 *(APP_{695}, Tau_{P301L}, $PS1_{M146V}$)*	Age-progressing memory impairment that	Age-dependent Aβ plaques, followed by the development of NFTs. Age-dependent synaptic dysfunction	(25,27)

Cognitive deficits: OR, object recognition; CFC, contextual fear conditioning; PPI, pre-pulse inhibition. Neuropathology: NFT, neurofibrillary tangle; CAA, congophilic amyloid angiopathy.

1.3 Magnetic resonance techniques in studies of Alzheimer's disease

Due to the importance of visualizing AD pathology *in vivo* to track disease progression and evaluate possible therapeutic interventions, much effort has focused in recent years on developing an imaging technique capable of accomplishing this. A major breakthrough in the imaging of AD has been the development of amyloid imaging tracers, such as the "Pittsburgh-B" compound, for positron emission tomography (36).

Although these markers allow visualization of plaque burden with PET in living AD patients (37), individual plaques with sizes ranging from 2-200 μm (14), are beyond the resolution of PET. Magnetic resonance imaging is an alternative imaging technique that should theoretically be able to reach the resolution necessary to visualize individual plaques, especially at high fields. An additional benefit of MRI is that it is a safer technique than PET as it does not require the use of ionizing radiation.

Presently various MR techniques that measure the anatomic, biochemical, microstructural, functional, and blood flow changes are being evaluated as possible surrogate measures of AD progression. MR based volumetry is being explored to detect anatomical changes and differentiate patients with AD from cognitive normal elderly (38), however, the validity of these MR-based volumetry for AD diagnosis remains to be established. Furthermore, volumetric imaging in transgenic mouse models of Alzheimer's disease is challenging due to the small size of the structures of interest in the brain and the low contrast between these structures. Although manual segmentation is still considered as the gold standard in morphometric studies, the variability in these findings is large (39). Consequently, relatively few studies on volumetric imaging in mice have been reported thus far. Efforts to image plaques using MRI are also underway. Over the last few years, multiple research groups have attempted to image Aβ plaque-load using MR microimaging (Table 1.2). For μMRI, strong magnetic field gradients and specialized radio frequency coils are used to generate images with higher spatial resolution than with normal MRI. Several studies involving μMRI of Aβ plaques *ex vivo* in human and *ex vivo* and *in vivo* in different transgenic mouse models of AD have been carried out with or without targeted contrast agents (Table 1.2). However, imaging of Aβ plaques *in vivo* still lacks sufficient sensitivity and requires further improvement. Another strategy to detect the presence of Aβ plaques in AD brain is to look for changes in MR relaxation rates which might be associated with the presence of Aβ. For instance, the transverse relaxation time of brain tissue might be modified due to the presence of iron in Aβ deposits (40). Functional MRI methods are being tested in an attempt to differentiate between AD patients and cognitively normal people. These methods measure differences in brain activation, such as visual saccades, visual and motor responses, semantic processing, angle discrimination, and memory (38). MR angiography is being investigated as a method to detect blood flow voids in transgenic mouse models of AD (41). Arterial spin labeling might aid in identifying blood flow reductions in AD patients relative to controls (42). MR spectroscopy is another MR-based technique that allows detection of biochemical changes in the brain and provides a noninvasive way to investigate *in vivo*

neurochemical abnormalities. MRS is being explored for detection of the altered neurochemical profile in AD brain (43). However, neurochemical changes that are specific only to AD have not yet been identified by MRS. A brief account of the development and future demands of MR imaging methods for Aβ plaque visualization, MR relaxometry and MRS for assessment of AD pathology is given below.

1.3.1 MRI to visualize Aβ plaques

Nearly a century after the first observation of plaques in post-mortem brain tissue by Alois Alzheimer in 1906, investigators are beginning to visualize Aβ plaques using MRI. MRI can provide much better resolution than SPECT or PET and can theoretically resolve individual plaques non-invasively. The first successful attempt to visualize plaques in fixed human tissue was achieved by Benveniste *et al.* in 1999 (44) using T_2*-weighted MRI at 7T with a spatial resolution in the range of 40×40×40 μm^3 (~6×10^{-5} mm^3). Plaques emerged as black, spherical elements on T_2* images, which can be attributed to the known presence of metals, particularly iron, in Aβ plaques (44). This finding was not replicated in another study, which reported the observed hypointensities to be vascular structures rather than Aβ plaques (45). Subsequently several types of transgenic mouse models of AD have also been used to visualize plaques in fixed mouse brain at different field strengths (4.7T, 7T, 9.4T). The scan times in these studies varied from ~60 min up to 15h. The best resolution achieved was 46×72×72 μm^3 using a spin echo sequence at 9.4T in 14h (46). Utilizing a fast spin echo sequence, plaque visualization was possible in 10-11 hours with a resolution of 54×58×200 μm^3 (47). Gradient echo sequences have been utilized for the *ex vivo* imaging of plaques in mouse brain that were stained with unspecific or target specific gadolinium based contrast agents (48,49).

Visualization of either plaque-load, or preferably individual plaques, in living human AD patients is an important goal of MRI studies in AD. However, current *in vivo* μMRI of Aβ plaques has only been successfully implemented in mouse models of AD, as the required field strengths are not yet widely available for human use. For the imaging of Aβ in mice, two distinct methods have been implemented: (i) methods using plaque specific gadolinium-, MION-, or ^{19}F-based contrast agents (50,51), and (ii) methods relying on the endogenous chemical properties of plaques to generate the desired contrast on MR images (8,52-54). The first reported study of *in vivo* plaque visualization in transgenic mice was by Wadghiri *et al.* in 2003 (51). This study was performed at 7T, using T_2 weighted SE and T_2* weighted GE sequences to obtain spatial resolutions of 59×59×500

μm and 59×59×250 μm^3, in scan times of 1-2 hrs. However, in this study the mice were administered different contrast agents prior to imaging, requiring a relatively invasive procedure. As a result longitudinal studies are generally not possible using this technique. In subsequent studies, Aβ plaques have been visualized in live mouse brain, without the need for an exogenous contrast agent (52,53). These studies were done at 9.4T with a spatial resolution of 60×60×120 μm^3 using a T_2 weighted SE sequence. However, imaging time was more than 1h and cardio-respiratory triggering was necessary to prevent motion artifacts (52,53). An overview of the described *in vivo* Aβ imaging studies is given in table 1.2. Despite these developments, plaque visualization still requires long measurement times, which makes it difficult to perform studies in human patients, or with a large number of animals. In addition, longitudinal MR studies to follow the development of plaques with age in the same animals have not been attempted in the above studies.

Table 1.2: MR imaging of Aβ plaques in humans and mouse models of Alzheimer disease.

Reference	Species	*in vivo/ ex vivo*	Contrast agent	MRI method	Field Strength	Image resolution	Imaging time
Benveniste *et al.* 1999 (44)	Human	*ex vivo*	-	3D T_2* GE; 3D DW SE	7T	5.9×10^{-5} mm^3	2.7-21.8 hr (GE) 4.6-18.2 hr (SE)
Dhenain *et al.* 2002 (45)	Human	*ex vivo*	-	T_2* GE	11.7T	46.9×23.4×23.4 μm^3 23.4×23.4×23.4 μm^3	16-18 hr
Poduslo *et al.* 2002 (49)	Mice: APP/PS1	*ex vivo*	PUT-Gd- Aβ	Not specified	7T	62.5×62.5×62.5 μm^3	~14 hr (T_1W) ~15 hr (T_2W)
Wadghiri *et al.* 2003 (51)	Mice: APP, APP/PS1	*in vivo; ex vivo*	Aβ-Gd; Aβ-MION	2D/3D T_1 SE; 2D T_2 SE; 2D T_2* GE	7T	59×59×500 μm^3 59×59×250 μm^3	120 min (T_2 SE) 59 min (T_2*GE)
Zhang *et al.* 2004 (46)	Mice: APP, APP/PS1	*ex vivo*	-	T_2 SE	9.4T	46×72×72 μm^3	14 hr
Lee *et al.* 2004 (47)	Mice: PS1, APP/PS1	*ex vivo*	-	T_2 FSE	7T	54×58×200 μm^3	65-80 min
Jack *et al.* 2004 (52)	Mice: APP/PS1	*in vivo; ex vivo*	-	T_2 SE; T_2* GE	9.4T	60×60×120 μm^3	67 min (SE) 87 min (GE)
Jack *et al.* 2005 (53)	Mice: APP/PS1	*in vivo; ex vivo*	-	T_2 SE	9.4T	60×60×120 μm^3 (30×30×60 μm^3)	100 min
Vanhoutte *et al.* 2005 (54)	Mice: APP$_{V717I}$	*in vivo*	-	3D T_2* GE	7T	78×156×234 μm^3 (78×78×58 μm^3)	68 min
Higuchi *et al.* 2005 (50)	Mice: Tg2576	*in vivo*	^{19}F -FSB	2D FSE; 3D FSE; T_1 GE	9.4T	156×156×500 μm^3	42 min
Dhenain *et al.* 2006 (48)	Mice: APP/PS1	*ex vivo*	-	3D T_2* GE	4.7T	63×47×59 μm^3	7-9 hr

2D/3D, 2- or 3-dimensional; T_1/T_2/T_2*, applied weighting in MR imaging experiments; DW, diffusion-weighted; ^{19}F, imaging of Fluorine-19 labeled contrast agent; GE, Gradient Echo; SE, Spin Echo; FSE, Fast Spin Echo.

1.3.2 MR relaxometry for the assessment of AD pathology

In addition to anatomical or pathological features, several intrinsic MR parameters can be studied to determine the effect of disease progression. In relaxometric approaches, the T_1 (longitudinal, or spin-lattice) and T_2 (transverse, or spin-spin) relaxation rates can be studied to facilitate the quantification of disease processes. T_1 specifies the rate at which the net magnetization returns to its equilibrium state along the axis of the magnet bore, while T_2 specifies the rate at which the net magnetization in the transverse plane returns to zero after RF excitation. Alternate relaxation parameters are T_2* and T_{1rho}; Unlike T_2, T_2* is influenced by magnetic field gradient inhomogeneities and is always shorter than the T_2 relaxation time. The spin lattice relaxation time constant in the rotating frame, T_{1rho}, determines the decay of the transverse magnetization in the presence of a "spin-lock" RF field (55).

Since both the T_2 and T_1 relaxation times are sensitive to changes in the biophysical water environment it has been hypothesized that the presence of increased deposition of Aβ in the brain affects these parameters (40). As such they might be used as independent markers for changes occurring in tissue, averaged over an ROI. Based on the findings reported thus far, T_2 relaxation appears to be more sensitive to pathophysiology than T_1 relaxation. Several groups have studied the effects of AD progression on the transverse relaxation rate T_2. There is converging evidence that the T_2 values of affected brain tissue are lower than in controls, and decrease as AD progresses (40,56,57). It has been proposed that a decrease of T_2 values provides evidence of early involvement of regional pathophysiological changes in the absence of neuronal cell loss in mouse brains exhibiting amyloid plaque neuropathology. The explicit influence of plaques on T_2 reduction is not yet clear. It has been proposed that the presence of iron in the plaques and/or cell shrinkage may be associated with decreased T_2 relaxation in plaque affected areas. Very recently, El Tannir El Tayara *et al.* have shown that T_2 relaxation can be affected by plaque deposition, without histochemically detectable iron (57). Furthermore, it has been proposed that a reduced cerebral blood flow resulting from amyloid deposition on vessel walls could contribute to the reduction in T_2 (40,56). A decrease of both T_2* and T_{1rho} values in plaque affected areas has been reported as well (54,55). An overview of recent relaxometry research in AD mouse models is presented in table 1.3. In most of these studies relaxation time and progressive Aβ deposition has been studied either at one time point or at various time points in different mice belonging to different age groups. A proper longitudinal MR study which follows both the development of Aβ plaques and changes in T_2 relaxation times with age in the same animals is lacking.

Table 1.3: Relaxometry measurements in AD mouse models

Reference	Relaxometric Parameter	AD mouse model	Remarks
Helpern *et al.* 2004 (40)	T_1, T_2	APP/PS1; PS1	T_2 lower in APP/PS1 and PS1 mice than in controls. No significant changes in T_1 detected.
Falangola *et al.* 2005 (58)	T_2	APP/PS1; PS1	T_2 decreased in APP/PS1 mice compared to controls
Vanhoutte *et al.* 2005 (54)	T_2*	APP_{V717I}	T_2* decreased in APP_{V717I} mice compared to controls
Borthakur *et al.* 2006 (55)	T_{1rho}	APP/PS1	T_{1rho} decreased after 12 months of age in APP/PS1 mice
El Tannir El Tayara *et al.* 2007 (57)	T_2	APP/PS1; PS1	T_2 decreased in amyloid loaded areas in APP/PS1 mice.
Falangola *et al.* 2007 (56)	T_2	APP/PS1; APP; PS1	Significant decrease in T_2 in APP and APP/PS1 mice. A longitudinal study*.

*several mice at each time point were measured longitudinally for T_2 measurements. However, as the experiment progressed, several of the mice that the experiment was started with were no longer included. To maintain a fixed number of animals, those that died between measurements were replaced with fresh ones.

1.3.3 MR spectroscopy of Alzheimer's disease

MRS is a noninvasive tool that can be used to measure the chemical composition of tissues *in vivo* and characterize functional metabolic processes in different parts of the body. In brain, MRS can provide a wealth of information on various facets of *in vivo* neurochemistry, including neuronal health, gliosis, osmoregulation, energy metabolism, neuronal-glial cycling, and molecular synthesis rates. A number of different nuclei can be observed using MR, and those that are most commonly seen in brain disorders - in decreasing order of number of studies - are ^{1}H, ^{31}P, ^{13}C, ^{19}F, ^{15}N, ^{23}Na, and ^{7}Li, with the first three accounting for approximately 99% of all studies. Of these, ^{1}H MRS is the most commonly applied in brain research, due to its higher sensitivity. At lower field strengths (1.5T and 3T), the number of metabolites that can be reliably quantified is relatively low. Metabolites that can be quantified include lactate, N-acetylaspartate, glutamate plus glutamine, creatine/phosphocreatine, choline-containing compounds, *myo*-inositol, and, in the rodent brain, taurine. Generally, little taurine is observed in primate brain, while in rodent brain taurine concentrations are quite high at ~5 mM. As with MRI, the current movement towards higher field strengths offers important advantages for MRS, because of the increase in signal-to-noise ratio coupled with the increase in spectral dispersion. This leads to easier identification of the many overlapping resonances. At much higher field strengths, such as 7T in humans and 9.4T in animals, it is possible to quantify an increased number of metabolites (59,60).

Both ^{1}H and ^{31}P NMR have been applied in the study of AD in humans. A decrease of NAA in AD has been reported in at least 18 studies, including *in vitro* studies showing a correlation with AD pathology (61,62). In addition to the decrease in NAA, numerous studies have shown an increase in *myo*-inositol in AD (63,64). The pathological significance of this increase in *myo*-inositol is not yet clear. It is possible that the increase is due to gliosis or osmoregulatory problems, and it has been inferred that it may be related to changes in osmoregulation (43). ^{31}P MRS studies of AD have shown abnormalities in the levels of membrane phospholipids and high energy metabolites that may depend on the severity of the illness (65).

In transgenic mouse models of AD, ^{1}H MRS has been applied in four different studies. In the first study Dedeoglu *et al.* studied Tg2576 mice using both *in vivo* MRS at 4.7T and *in vitro* MRS at 11.7T (66). The data revealed decreased NAA and Glu, and increased taurine levels compared with the wild-type controls. In addition, they were able to detect a decrease in GSH from spectra *in vitro*. A second MRS study examined another model of AD: the APP/PS2 model. APP/PS2 mice showed a similar age-dependent decrease in NAA and Glu. A correlation with the plaque burden in 24-month-old animals was found, with little spectroscopic abnormalities before 16 months of age (67). The third MRS study examined the age-dependent spectroscopic changes noted in yet another mouse model of AD, the so-called APP/PS1 model. APP/PS1 mice start to develop plaques at an earlier age than the single transgene APP mice. In the APP/PS1 model, there was an age-dependent increase in *myo*-inositol and decreases in NAA and Glu were detected. The changes in *myo*-inositol were only significant after about 400 days of age (68). The observation of increased *myo*-inositol in APP/PS1 mice was very different from those made in the previous studies using APP and APP/PS2 mice. APP mice showed an increase in tau rather than *myo*-inositol and changes in neither *myo*-inositol nor taurine were reported in APP/PS2 mice. However, the increase in *myo*-inositol is consistent with observations in human AD studies. Marjanska *et al.* proposed that the ratio of NAA and *myo*-inositol might be a sensitive spectroscopic marker for following AD in human disease as well as in mouse models such as the APP/PS1 (68). However, if NAA and *myo*-inositol represent two different pathological mechanisms coupled to cellular processes in different cellular compartments, they can have independent temporal profiles as the disease progresses, and the ratio may mask this. For instance, in the study of APP/PS1 mice (68), NAA appears to decline fairly linearly with age, while the *myo*-inositol does not show an increase until after 400 days of age. This may reflect different roles and cellular compartments of NAA and *myo*-inositol, the former being primarily

neuronal and the latter glial (68). The fourth study examined 3xTgAD mice, and it was found that at 6 months of age NAA was already declining, while changes in other metabolite levels were not reported (43).

Although a decrease in NAA and an increase in either *myo*-inositol or taurine has been consistently observed in AD, these changes are not specific to only AD, since they have been shown to occur in other neurodegenerative diseases such as Huntington's disease, Parkinson's disease as well as in other brain disorders (43,69,70). Therefore, specific *in vivo* MRS markers of AD are still missing. While transgenic mouse models of AD might be instrumental in discovering new *in vivo* biomarkers of AD, the use of localized *in vivo* 1D MRS in mice is often hampered by low sensitivity of local measurements due to both the small size of the brain resulting in limited signal-to-noise ratio and low concentrations of several brain metabolites. Important neurotransmitters and other metabolites cannot be reliably distinguished due to overlapping or merging of their respective peaks in 1D MRS, although the recent development of high field magnets suitable for *in vivo* investigations in small animals has partly overcome this limitation. However, even with high-field magnets, the spectral dispersion in the proton spectra is limited, since most of the metabolites appear in a narrow spectral range of 5 ppm. Due to local field inhomogeneities in the small mouse brain, signals are broad (10-20 Hz), which results in a considerable overlap of resonances of numerous metabolites, especially those from coupled spin systems (71). Thus, ambiguity in assignment in 1D MRS is unavoidable for localized *in vivo* studies, especially in mouse brain. While 1D spectra at high magnetic field can yield accurate quantification of the known metabolites using analysis software such as LCmodel, which uses a linear combination of model spectra from a predefined basis set to simulate the measured spectra (72), unexpected metabolites are easily overlooked.

Spectral editing MRS sequences offer the possibility to resolve specific metabolites from overlapping regions in the spectra, thus facilitating their unambiguous resonance assignment and characterization *in vivo*. However, this requires pre-selection of metabolites of interest and only a single selected metabolite can be detected per measurement. A correct assignment of metabolite resonances *in vivo* is essential for their quantification under normal and various pathophysiological conditions and for identifying potential biomarkers of various brain disorders, including AD.

Compared to localized 1D MRS, localized 2D ^{1}H MRS overcomes the problem of spectral overlap considerably, as the resonances are dispersed over a two-dimensional surface, allowing the separation and unambiguous assignment of resonances of several metabolites in a single measurement. Recently several 2D MRS sequences have been proposed and implemented for studying brain metabolism in human subjects, using clinical MRI scanners (71,73,74). The techniques based on localized variations of the COSY sequence appear most promising with regards to identifying metabolites that are unresolved in 1D MRS sequences due to spectral crowding. With regards to 2D MRS in small animal models, there have been a few reports of localized 2D MRS performed on rat brains (75,76), but thus far 2D MRS studies in the brains of mice have not yet been reported.

1.4 Thesis scope

The rapidly expanding range of MR techniques for imaging neuropathologies and non-invasively assessing neurochemistry *in vivo*, in parallel with the rapid development of transgenic mouse models, offers great potential for the discovery of novel biomarkers of disease progression. Presently no definitive *in vivo* biomarker of AD is available, which impedes both clinical diagnosis in humans and drug discovery in transgenic animal models. Non-invasive rapid visualization of Aβ plaque pathology and identification of new *in vivo* early biomarkers of AD using the various MR based techniques in transgenic mouse models of AD would not only facilitate intervention and enhance treatment success but would also contribute to understanding the mechanism of Alzheimer's disease. The *in vivo* μMRI approaches used for Aβ plaque visualization thus far need further improvements in resolution and reduction in scan times. Furthermore, longitudinal MR studies which follow plaque development are required, to study plaque biology and its effects in the same animals as they age. In addition, longitudinal MR studies may prove beneficial for assessing the efficacy of amyloid reduction therapies currently under intense development by major pharmaceutical companies.

In addition to the use of Aβ plaque imaging, some of the intrinsic MR parameters such as T_2 relaxation times, which are sensitive to changes in the biophysical environment of water in tissues, may be applied as a sensitive marker for detecting early changes in Alzheimer's brain. These changes can be followed with time in longitudinal studies to identify correlations between plaque development and T_2 relaxation times. Another possibility for identifying potential early biomarkers of AD is the application of *in vivo* localized magnetic resonance spectroscopy to study neurochemical changes resulting

from the disease. As described in the previous section, a major concern with one-dimensional MRS is that there is strong signal overlap which can make identification and precise quantification difficult, in particular for metabolites with coupled spin systems. Better signal dispersion, easier assignment and more accurate quantification can be achieved by the combination of: a) high magnetic field, since the dispersion of chemical shifts increases with magnetic field strength and b) localized 2D MR techniques, since the added dimension in a localized 2D MR spectrum yields an improved spectral resolution compared to conventional 1D MR spectra. In addition to unambiguous assignment opportunities of the various known neurometabolites *in vivo*, 2D MRS has great potential for resolving the resonances of brain metabolites at low concentration that are hidden by overlapping signals. This may be extremely beneficial in future studies, and significantly aid in detecting new biomarkers of the various neurodegenerative diseases, including AD. However, as previously mentioned, 2D MRS has thus far not been applied in studies using mouse models of disease. The specific aim of this thesis is to implement and optimize high resolution MR imaging methods to follow longitudinally the AD pathology in transgenic mouse models of AD, to optimize localized 2D MRS methods for the mouse brain, and to map the neurochemical composition of the brain of AD transgenic mice using high resolution 2D MRS.

Chapter 2 of this thesis presents the basic theoretical background behind MRI and 1D/2D MRS techniques. In **chapter 3**, high-field μMRI methods have been optimized and successfully implemented to visualize Aβ plaques in the Tg2576 transgenic mouse model of AD, and to follow Aβ plaque development in the same transgenic mice with age. Additionally, the T_2 relaxation times were studied as the mice aged, to study how AD progression and Aβ plaque deposition influence the MR relaxometric properties of brain tissue. Described in **chapter 4** is the implementation and optimization of a localized 2D MR spectroscopic sequence, L-COSY, at 9.4T. Using this sequence, highly resolved 2D MR spectra were obtained, for the first time, from localized regions in the mouse brain *in vivo*. In **chapter 5**, two-dimensional MRS is applied to study the age-dependent metabolic changes in the brain of Tg2576 mice and correlate these changes with the severity of plaque deposition as observed by μMRI. **Chapter 6** provides a general discussion to the work presented in this thesis, and presents some future prospects.

References

1. Price JL, Davis PB, Morris JC, White DL. The Distribution Of Tangles, Plaques And Related Immunohistochemical Markers In Healthy Aging And Alzheimers-Disease. Neurobiol Aging 1991;12:295-312.
2. Terry RD, Masliah E, Salmon DP, Butters N, Deteresa R, Hill R, Hansen LA, Katzman R. Physical Basis Of Cognitive Alterations In Alzheimers-Disease - Synapse Loss Is The Major Correlate Of Cognitive Impairment. Ann Neurol 1991;30:572-580.
3. Burdick D, Soreghan B, Kwon M, Kosmoski J, Knauer M, Henschen A, Yates J, Cotman C, Glabe C. Assembly And Aggregation Properties Of Synthetic Alzheimers A4/Beta Amyloid Peptide Analogs. J Biol Chem 1992;267:546-554.
4. McGowan E, Eriksen J, Hutton M. A decade of modeling Alzheimer's disease in transgenic mice. Trends In Genetics 2006;22:281-289.
5. Petrella JR. Neuroimaging and early diagnosis of Alzheimer disease: A look to the future (vol 226, pg 315, 2003). Radiology 2003;227:613-613.
6. Gravina SA, Ho LB, Eckman CB, Long KE, Otvos L, Younkin LH, Suzuki N, Younkin SG. Amyloid-Beta Protein (A-Beta) In Alzheimers-Disease Brain - Biochemical And Immunocytochemical Analysis With Antibodies Specific For Forms Ending At A-Beta-40 Or A-Beta-42(43). J Biol Chem 1995;270:7013-7016.
7. Hardy J, Selkoe DJ. Medicine - The amyloid hypothesis of Alzheimer's disease: Progress and problems on the road to therapeutics. Science 2002;297:353-356.
8. Jack CR, Marjanska M, Wengenack TM, Reyes DA, Curran GL, Lin J, Preboske GM, Poduslo JF, Garwood M. Magnetic resonance imaging of Alzheimer's pathology in the brains of living transgenic mice: A new tool in Alzheimer's disease research. Neuroscientist 2007;13:38-48.
9. Cleary JP, Walsh DM, Hofmeister JJ, Shankar GM, Kuskowski MA, Selkoe DJ, Ashe KH. Natural oligomers of the amyloid-protein specifically disrupt cognitive function. Nat Neurosci 2005;8:79-84.
10. Spires TL, Meyer-Luehmann M, Stern EA, McLean PJ, Skoch J, Nguyen PT, Bacskai BJ, Hyman BT. Dendritic spine abnormalities in amyloid precursor protein transgenic mice demonstrated by gene transfer and intravital multiphoton microscopy. J Neurosci 2005;25:7278-7287.
11. Tsai J, Grutzendler J, Duff K, Gan WB. Fibrillar amyloid deposition leads to local synaptic abnormalities and breakage of neuronal branches. Nat Neurosci 2004;7:1181-1183.

12. Lewis J, Dickson DW, Lin WL, Chisholm L, Corral A, Jones G, Yen SH, Sahara N, Skipper L, Yager D, Eckman C, Hardy J, Hutton M, McGowan E. Enhanced neurofibrillary degeneration in transgenic mice expressing mutant tau and APP. Science 2001;293:1487-1491.
13. SantaCruz K, Lewis J, Spires T, Paulson J, Kotilinek L, Ingelsson M, Guimaraes A, DeTure M, Ramsden M, McGowan E, Forster C, Yue M, Orne J, Janus C, Mariash A, Kuskowski M, Hyman B, Hutton M, Ashe KH. Tau suppression in a neurodegenerative mouse model improves memory function. Science 2005;309:476-481.
14. Lehericy S, Marjanska M, Mesrob L, Sarazin M, Kinkingnehun S. Magnetic resonance imaging of Alzheimer's disease. European Radiology 2007;17:347-362.
15. Wengenack TM, Whelan S, Curran GL, Duff KE, Poduslo JF. Quantitative histological analysis of amyloid deposition in Alzheimer's double transgenic mouse brain. Neuroscience 2000;101:939-944.
16. Geula C. Pathological diagnosis of Alzheimer’s disease. In: The early diagnosis of Alzheimer’s disease. Totowa, NJ: Humana, 2000; 65–82.
17. Braak H, Braak E. Neuropathological Staging Of Alzheimer-Related Changes. Acta Neuropathol 1991;82:239-259.
18. Holcomb L, Gordon MN, McGowan E, Yu X, Benkovic S, Jantzen P, Wright K, Saad I, Mueller R, Morgan D, Sanders S, Zehr C, O'Campo K, Hardy J, Prada CM, Eckman C, Younkin S, Hsiao K, Duff K. Accelerated Alzheimer-type phenotype in transgenic mice carrying both mutant amyloid precursor protein and presenilin 1 transgenes. Nat Med 1998;4:97-100.
19. Hsiao K, Chapman P, Nilsen S, Eckman C, Harigaya Y, Younkin S, Yang FS, Cole G. Correlative memory deficits, A beta elevation, and amyloid plaques in transgenic mice. Science 1996;274:99-102.
20. Wengenack TM, Curran GL, Poduslo JF. Targeting Alzheimer amyloid plaques in vivo. Nat Biotechnol 2000;18:868-872.
21. Irizarry MC, McNamara M, Fedorchak K, Hsiao K, Hyman BT. APP(Sw) transgenic mice develop age-related A beta deposits and neuropil abnormalities, but no neuronal loss in CA1. J Neuropathol Exp Neurol 1997;56:965-973.
22. Irizarry MC, Soriano F, McNamara M, Page KJ, Schenk D, Games D, Hyman BT. A beta deposition is associated with neuropil changes, but not with overt neuronal loss in the human amyloid precursor protein V717F (PDAPP) transgenic mouse. J Neurosci 1997;17:7053-7059.

23. Allen B, Ingram E, Takao M, Smith MJ, Jakes R, Virdee K, Yoshida H, Holzer M, Craxton M, Emson PC, Atzori C, Migheli A, Crowther RA, Ghetti B, Spillantini MG, Goedert M. Abundant tau filaments and nonapoptotic neurodegeneration in transgenic mice expressing human P301S tau protein. J Neurosci 2002;22:9340-9351.
24. Lewis J, McGowan E, Rockwood J, Melrose H, Nacharaju P, Van Slegtenhorst M, Gwinn-Hardy K, Murphy MP, Baker M, Yu X, Duff K, Hardy J, Corral A, Lin WL, Yen SH, Dickson DW, Davies P, Hutton M. Neurofibrillary tangles, amyotrophy and progressive motor disturbance in mice expressing mutant (P301L) tau protein. Nature Genet 2000;25:402-405.
25. Oddo S, Caccamo A, Shepherd JD, Murphy MP, Golde TE, Kayed R, Metherate R, Mattson MP, Akbari Y, LaFerla FM. Triple-transgenic model of Alzheimer's disease with plaques and tangles: Intracellular A beta and synaptic dysfunction. Neuron 2003;39:409-421.
26. Perez M, Ribe E, Rubio A, Lim F, Moran MA, Ramos PG, Ferrer I, Isla MTG, Avila J. Characterization of a double (amyloid precursor protein-tau) transgenic: Tau phosphorylation and aggregation. Neuroscience 2005;130:339-347.
27. Oddo S, Caccamo A, Kitazawa M, Tseng BP, LaFerla FM. Amyloid deposition precedes tangle formation in a triple transgenic model of Alzheimer's disease. Neurobiol Aging 2003;24:1063-1070.
28. Oddo S, Caccamo A, Tran L, Lambert MP, Glabe CG, Klein WL, LaFerla FM. Temporal profile of amyloid-beta (A beta) oligomerization in an in vivo model of Alzheimer disease - A link between A beta and tau pathology. J Biol Chem 2006;281:1599-1604.
29. Sturchler-Pierrat C, Abramowski D, Duke M, Wiederhold KH, Mistl C, Rothacher S, Ledermann B, Burki K, Frey P, Paganetti PA, Waridel C, Calhoun ME, Jucker M, Probst A, Staufenbiel M, Sommer B. Two amyloid precursor protein transgenic mouse models with Alzheimer disease-like pathology. Proc Natl Acad Sci U S A 1997;94:13287-13292.
30. Duff K, Eckman C, Zehr C, Yu X, Prada CM, Pereztur J, Hutton M, Buee L, Harigaya Y, Yager D, Morgan D, Gordon MN, Holcomb L, Refolo L, Zenk B, Hardy J, Younkin S. Increased amyloid-beta 42(43) in brains of mice expressing mutant presenilin 1. Nature 1996;383:710-713.

31. Borchelt DR, Ratovitski T, vanLare J, Lee MK, Gonzales V, Jenkins NA, Copeland NG, Price DL, Sisodia SS. Accelerated amyloid deposition in the brains of transgenic mice coexpressing mutant presenilin 1 and amyloid precursor proteins. Neuron 1997;19:939-945.
32. Tanemura K, Akagi T, Murayama M, Kikuchi N, Murayama O, Hashikawa T, Yoshiike Y, Park JM, Matsuda K, Nakao S, Sun XY, Sato S, Yamaguchi H, Takashima A. Formation of filamentous tau aggregations in transgenic mice expressing V337M human tau. Neurobiol Dis 2001;8:1036-1045.
33. Tatebayashi Y, Miyasaka T, Chui DH, Akagi T, Mishima K, Iwasaki K, Fujiwara M, Tanemura K, Murayama M, Ishiguro K, Planel E, Sato S, Hashikawa T, Takashima A. Tau filament formation and associative memory deficit in aged mice expressing mutant (R406W) human tau. Proc Natl Acad Sci U S A 2002;99:13896-13901.
34. Ramsden M, Kotilinek L, Forster C, Paulson J, McGowan E, SantaCruz K, Guimaraes A, Yue M, Lewis J, Carlson G, Hutton M, Ashe KH. Age-dependent neurofibrillary tangle formation, neuron loss, and memory impairment in a mouse model of human tauopathy (P301L). J Neurosci 2005;25:10637-10647.
35. Andorfer C, Kress Y, Espinoza M, de Silva R, Tucker KL, Barde YA, Duff K, Davies P. Hyperphosphorylation and aggregation of tau in mice expressing normal human tau isoforms. J Neurochem 2003;86:582-590.
36. Klunk WE, Engler H, Nordberg A, Wang YM, Blomqvist G, Holt DP, Bergstrom M, Savitcheva I, Huang GF, Estrada S, Ausen B, Debnath ML, Barletta J, Price JC, Sandell J, Lopresti BJ, Wall A, Koivisto P, Antoni G, Mathis CA, Langstrom B. Imaging brain amyloid in Alzheimer's disease with Pittsburgh Compound-B. Ann Neurol 2004;55:306-319.
37. Sair HI, Doraiswamy PM, Petrella JR. In vivo amyloid imaging in Alzheimer's disease. Neuroradiology 2004;46:93-104.
38. Kantarci K, Jack CR. Neuroimaging in Alzheimer disease: An evidence-based review. Neuroimaging Clin N Am 2003;13:197-209.
39. Bookstein FL. "Voxel-based morphometry" should not be used with imperfectly registered images. Neuroimage 2001;14:1454-1462.
40. Helpern JA, Lee SP, Falangola MF, Dyakin VV, Bogart A, Ardekani B, Duff K, Branch C, Wisniewski T, de Leon MJ, Wolf O, O'Shea J, Nixon RA. MRI assessment of neuropathology in a transgenic mouse model of Alzheimer's disease. Magn Reson Med 2004;51:794-798.

41. Beckmann N, Schuler A, Mueggler T, Meyer EP, Wiederhold KH, Staufenbiel M, Krucker T. Age-dependent cerebrovascular abnormalities and blood flow disturbances in APP23 mice modeling Alzheimer's disease. J Neurosci 2003;23:8453-8459.
42. Alsop DC, Detre JA, Grossman M. Assessment of cerebral blood flow in Alzheimer's disease by spin-labeled magnetic resonance imaging. Ann Neurol 2000;47:93-100.
43. Choi JK, Dedeoglu A, Jenkins BG. Application of MRS to mouse models of neurodegenerative illness. NMR Biomed 2007;20:216-237.
44. Benveniste H, Einstein G, Kim KR, Hulette C, Johnson A. Detection of neuritic plaques in Alzheimer's disease by magnetic resonance microscopy. Proc Natl Acad Sci U S A 1999;96:14079-14084.
45. Dhenain M, Privat N, Duyckaerts C, Jacobs RE. Senile plaques do not induce susceptibility effects in T_2*-weighted MR microscopic images. NMR Biomed 2002;15:197-203.
46. Zhang J, Yarowsky P, Gordon MN, Di Carlo G, Munireddy S, van Zijl PCM, Mori S. Detection of amyloid plaques in mouse models of Alzheimer's disease by magnetic resonance imaging. Magn Reson Med 2004;51:452-457.
47. Lee SP, Falangola MF, Nixon RA, Duff K, Helpern JA. Visualization of beta-amyloid plaques in a transgenic mouse model of Alzheimer's disease using MR microscopy without contrast reagents. Magn Reson Med 2004;52:538-544.
48. Dhenain M, Delatour B, Walczak C, Volk A. Passive staining: A novel ex vivo MRI protocol to detect amyloid deposits in mouse models of Alzheimer's disease. Magn Reson Med 2006;55:687-693.
49. Poduslo JF, Wengenack TM, Curran GL, Wisniewski T, Sigurdsson EM, Macura SI, Borowski BJ, Jack CR. Molecular targeting of Alzheimer's amyloid plaques for contrast-enhanced magnetic resonance imaging. Neurobiol Dis 2002;11:315-329.
50. Higuchi M, Iwata N, Matsuba Y, Sato K, Sasamoto K, Saido TC. ^{19}F and ^{1}H MRI detection of amyloid beta plaques in vivo. Nat Neurosci 2005;8:527-533.
51. Wadghiri YZ, Sigurdsson EM, Sadowski M, Elliott JI, Li YS, Scholtzova H, Tang CY, Aguinaldo G, Pappolla M, Duff K, Wisniewski T, Turnbull DH. Detection of Alzheimer's amyloid in Transgenic mice using magnetic resonance microimaging. Magn Reson Med 2003;50:293-302.

52. Jack CR, Garwood M, Wengenack TM, Borowski B, Curran GL, Lin J, Adriany G, Grohn IHJ, Grimm R, Poduslo JF. In vivo visualization of Alzheimer's amyloid plaques by magnetic resonance imaging in transgenic mice without a contrast agent. Magn Reson Med 2004;52:1263-1271.
53. Jack CR, Wengenack TM, Reyes DA, Garwood M, Curran GL, Borowski BJ, Lin J, Preboske GM, Holasek SS, Adriany G, Poduslo JF. In vivo magnetic resonance microimaging of individual amyloid plaques in Alzheimer's transgenic mice. J Neurosci 2005;25:10041-10048.
54. Vanhoutte G, Dewachter I, Borghgraef P, Van Leuven F, Van der Linden A. Noninvasive in vivo MRI detection of neuritic plaques associated with iron in APP[V717I] transgenic mice, a model for Alzheimer's disease. Magn Reson Med 2005;53:607-613.
55. Borthakur A, Gur T, Wheaton AJ, Corbo M, Trojanowski JQ, Lee VMY, Reddy R. In vivo measurement of plaque burden in a mouse model of Alzheimer's disease. J Magn Reson Imaging 2006;24:1011-1017.
56. Falangola MF, Dyakin VV, Lee SP, Bogart A, Babb JS, Duff K, Nixon R, Helpern JA. Quantitative MRI reveals aging-associated T_2 changes in mouse models of Alzheimer's disease. NMR Biomed 2007;20:343-351.
57. El Tayara NET, Volk A, Dhenain M, Delatour B. Transverse relaxation time reflects brain amyloidosis in young APP/PS1 transgenic mice. Magn Reson Med 2007;58:179-184.
58. Falangola MF, Ardekani BA, Lee SP, Babb JS, Bogart A, Dyakin VV, Nixon R, Duff K, Helpern JA. Application of a non-linear image registration algorithm to quantitative analysis of T_2 relaxation time in transgenic mouse models of AD pathology. J Neurosci Methods 2005;144:91-97.
59. Pfeuffer J, Tkac I, Provencher SW, Gruetter R. Toward an in vivo neurochemical profile: Quantification of 18 metabolites in short-echo-time H-1 NMR spectra of the rat brain. J Magn Reson 1999;141:104-120.
60. Tkac I, Andersen P, Adriany G, Merkle H, Ugurbil K, Gruetter R. In vivo H-1 NMR spectroscopy of the human brain at 7 T. Magn Reson Med 2001;46:451-456.
61. Klunk WE, Xu C, Panchalingam K, McClure RJ, Pettegrew JW. Quantitative H-1 and P-31 MRS of PCA extracts of postmortem Alzheimer's disease brain. Neurobiol Aging 1996;17:349-357.

62. Mohanakrishnan P, Fowler AH, Vonsattel JP, Husain MM, Jolles PR, Liem P, Komoroski RA. An In-Vitro H-1 Nuclear-Magnetic-Resonance Study Of The Temporoparietal Cortex Of Alzheimer Brains. Exp Brain Res 1995;102:503-510.
63. Jessen F, Block W, Traber F, Keller E, Flacke S, Papassotiropoulos A, Lamerichs R, Heun R, Schild HH. Proton MR spectroscopy detects a relative decrease of N-acetylaspartate in the medial temporal lobe of patients with AD. Neurology 2000;55:684-688.
64. Miller BL. A Review Of Chemical Issues In H-1-Nmr Spectroscopy - N-Acetyl-L-Aspartate, Creatine And Choline. NMR Biomed 1991;4:47-52.
65. Pettegrew JW, Panchalingam K, Moossy J, Martinez J, Rao G, Boller F. Correlation Of P-31 Magnetic-Resonance Spectroscopy And Morphologic Findings In Alzheimers-Disease. Arch Neurol 1988;45:1093-1096.
66. Dedeoglu A, Choi JK, Cormier K, Kowall NW, Jenkins BG. Magnetic resonance spectroscopic analysis of Alzheimer's disease mouse brain that express mutant human APP shows altered neurochemical profile. Brain Res 2004;1012:60-65.
67. von Kienlin M, Kunnecke B, Metzger F, Steiner G, Richards JG, Ozmen L, Jacobsen H, Loetscher H. Altered metabolic profile in the frontal cortex of PS2APP transgenic mice, monitored throughout their life span. Neurobiol Dis 2005;18:32-39.
68. Marjanska M, Curran GL, Wengenack TM, Henry PG, Bliss RL, Poduslo JF, Jack CR, Ugurbil K, Garwood M. Monitoring disease progression in transgenic mouse models of Alzheimer's disease with proton magnetic resonance spectroscopy. Proc Natl Acad Sci U S A 2005;102:11906-11910.
69. Tsang TA, Woodman B, McLoughlin GA, Griffin JL, Tabrizi SJ, Bates GP, Holmes E. Metabolic characterization of the R6/2 transgenic mouse model of Huntington's disease by high-resolution MAS H-1 NMR spectroscopy. J Proteome Res 2006;5:483-492.
70. Boska MD, Lewis TB, Destache CJ, Benner EJ, Nelson JA, Uberti M, Mosley RL, Gendelman HE. Quantitative H-1 magnetic resonance spectroscopic imaging determines therapeutic immunization efficacy in an animal model of Parkinson's disease. J Neurosci 2005;25:1691-1700.
71. Thomas MA, Yue K, Binesh N, Davanzo P, Kumar A, Siegel B, Frye M, Curran J, Lufkin R, Martin P, Guze B. Localized two-dimensional shift correlated MR spectroscopy of human brain. Magn Reson Med 2001;46:58-67.
72. Provencher SW. Estimation Of Metabolite Concentrations From Localized In-Vivo Proton Nmr-Spectra. Magn Reson Med 1993;30:672-679.

73. Thomas MA, Hattori N, Umeda M, Sawada T, Naruse S. Evaluation of two-dimensional L-COSY and PRESS using a 3 T MRI scanner: from phantoms to human brain in vivo. NMR Biomed 2003;16:245-251.
74. Binesh N, Yue K, Fairbanks L, Thomas MA. Reproducibility of localized 2D correlated MR spectroscopy. Magn Reson Med 2002;48:942-948.
75. Delmas F, Beloeil JC, van der Sanden BPJ, Nicolay K, Gillet B. Two-voxel localization sequence for in vivo two-dimensional homonuclear correlation spectroscopy. J Magn Reson 2001;149:119-125.
76. Welch JWR, Bhakoo K, Dixon RM, Styles P, Sibson NR, Blamire AM. In vivo monitoring of rat brain metabolites during vigabatrin treatment using localized 2D-COSY. NMR Biomed 2003;16:47-54.